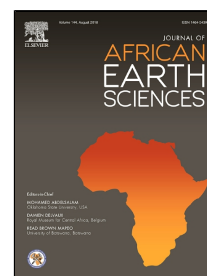


Accepted Manuscript

Chemistry of volcanic soils used for agriculture in Brava Island (Cape Verde) envisaging a sustainable management

Rosa Marques, Bruno J. Vieira, M.Isabel Prudêncio, João C. Waerenborgh, M. Isabel Dias, Fernando Rocha



PII: S1464-343X(18)30168-7
DOI: 10.1016/j.jafrearsci.2018.06.014
Reference: AES 3240
To appear in: *Journal of African Earth Sciences*
Received Date: 17 January 2018
Accepted Date: 11 June 2018

Please cite this article as: Rosa Marques, Bruno J. Vieira, M.Isabel Prudêncio, João C. Waerenborgh, M.Isabel Dias, Fernando Rocha, Chemistry of volcanic soils used for agriculture in Brava Island (Cape Verde) envisaging a sustainable management, *Journal of African Earth Sciences* (2018), doi: 10.1016/j.jafrearsci.2018.06.014

This is a PDF file of an unedited manuscript that has been accepted for publication. As a service to our customers we are providing this early version of the manuscript. The manuscript will undergo copyediting, typesetting, and review of the resulting proof before it is published in its final form. Please note that during the production process errors may be discovered which could affect the content, and all legal disclaimers that apply to the journal pertain.

1 **Chemistry of volcanic soils used for agriculture in Brava Island (Cape Verde) envisaging**
2 **a sustainable management**

3

4 Rosa Marques^{a*}, Bruno J. Vieira^a, M. Isabel Prudêncio^a, João C. Waerenborgh^a, M. Isabel Dias^a,
5 Fernando Rocha^{b,c}

6 ^aCentro de Ciências e Tecnologias Nucleares (C2TN), Instituto Superior Técnico, Universidade de
7 Lisboa, EN 10 (km 139.7), 2695-066 Bobadela, Portugal

8 ^bGeoBioTec, Universidade de Aveiro, Campus Universitário Santiago, 3810-193 Aveiro, Portugal

9 ^cDep. de Geociências, Universidade de Aveiro, Campus Universitário Santiago, 3810-193 Aveiro,
10 Portugal

11 * Corresponding author (rmarques@ctn.tecnico.ulisboa.pt)

12 brunovieira@ctn.tecnico.ulisboa.pt (Bruno J. Vieira)

13 iprudenc@ctn.tecnico.ulisboa.pt (M. Isabel Prudêncio)

14 jcarlos@ctn.tecnico.ulisboa.pt (João C. Waerenborgh)

15 isadias@ctn.tecnico.ulisboa.pt (M. Isabel Dias)

16 tavares.rocha@ua.pt (Fernando Rocha)

17

18 **Abstract**

19 In order to acquire a better knowledge of iron forms, clay minerals and the content and distribution of
20 trace elements in soils mostly used for agriculture in the semi-arid Brava Island (Cape Verde), iron
21 speciation, mineralogy and chemical contents in the clay-size fraction (< 2 µm) of incipient soils
22 developed on sediments and phonolitic pyroclasts was performed by Mössbauer spectroscopy, X-ray
23 diffraction and neutron activation analysis. In contrast with the whole samples in the clay-size fraction
24 of all the studied soils only Fe(III) was detected. Iron and chromium are depleted suggesting their
25 occurrence as ferromagnesian and oxide minerals present in coarser particles. Rare earth elements are
26 concentrated in the clay-size fraction, and significant differences are found in their distribution which
27 may be partially due to oxidation, since Ce anomalies were observed. Among the other chemical
28 elements studied, high concentrations of arsenic, bromine, and particularly antimony were found in the
29 clay-size fraction of soils where all the Fe oxides are nano-sized, confirming the predominant
30 adsorption of these elements on the nano-particles surface. The existence of significant amounts of

31 these elements as well as of vitreous phases in fine particles of these soils may contribute to their
32 mobility and accumulation in groundwater and in plants, both by absorption and by dust deposition
33 onto the plant leaves.

34

35 **Keywords:** Brava Island; Cape Verde; Volcanic soil; REE; Trace elements; Iron speciation

36

37 **1. Introduction**

38 The knowledge of arid zone soils has become increasingly important since global warming has
39 worsened the water resource crisis in many zones worldwide from Africa to Asia (Han, 2007).

40 Volcanic eruptions form part of the biogeochemical cycle of the elements and represent one of the
41 natural ways in which significant amounts of chemical elements enter the atmosphere (Nriagu, 1989).

42 The environmental impact of ash deposits, which contribute with considerable quantities of metals to
43 sediments and soils, is also of the utmost relevance. As shown by several studies, major, minor and
44 trace elements can quickly transfer from ash into the environment, leading to considerably high
45 concentration of these elements in water and vegetation (Cronin et al., 2003; Frogner et al., 2001;
46 Jones and Gislason, 2008; Martin et al., 2009; Watt et al., 2009). Thus, soils with contribution from
47 volcanic eruptions, particularly those developed on oceanic volcanic islands, may have significant
48 amounts of a number of chemical elements. Volcanic soils are rich in mineral nutrients being amongst
49 the most fertile lands in the world and are intensively cultivated. Nevertheless they may have an
50 imbalance of chemical elements that can impact on the health of plants and animals growing in or on
51 the soils (Neall, 2007). This may be particularly relevant in the case of volcanic islands of recent and
52 contrasting volcanism that are under semi-arid climate, which is the case of Cape Verde.

53 The Cape Verde archipelago is located in the Atlantic Ocean. The semi-arid climate of these
54 islands gives rise to topsoils with low to moderate degree of weathering and development, in general
55 with less than 30 cm depth. Although Brava is one of the islands with more frequent rainy periods in
56 Cape Verde, the aridity associated with the rough topography leads to incipient soils (Madeira and
57 Ricardo, 2013). Nevertheless, soils of alluviums and colluviums, the major areas for agriculture, can

58 be found in valleys. Furthermore, high contents of trace elements may occur originated from
59 imbalance of elements in the volcanic parent materials, which may be a threat to the environmental
60 health (Marques et al., 2012, 2014a, 2014b, 2016, 2017a, 2017b, 2017c). Detailed Fe speciation and
61 chemical composition studies of Cape Verde soils, namely of Fogo and Brava Islands (Marques et al.,
62 2014b, 2016, 2017c) have shown that oxidation is a major weathering mechanism. The global iron
63 oxidation appears to be a good indicator of the weathering degree in these semi-arid islands. In
64 addition to information on pedogenetic conditions Fe oxides may affect a number of soil properties,
65 namely surface adsorption of numerous ions and molecules. Significant chemical content variations
66 were found to occur as well as high contents of Mn, Co, Ga, Ba, rare earth elements (REE), Ta, W, Th
67 and U in the whole sample ($\phi < 2$ mm) of soils (Marques et al., 2016). These results justify a more
68 detailed study concerning fine particles, which have the highest surface areas, of soils used for
69 agriculture in Brava, a crucial resource of this small island.

70 The soils mostly used for agriculture in Brava Island are those developed on phonolitic
71 pyroclasts and sediments on a plateau between 300 and 976 m above sea level, and also on sediments
72 occurring on terraces of fluvial incisions of the steep coastal cliffs (Fig. 1). In this work the clay-size
73 fraction ($\phi < 2$ μm) of these soils were analysed by Mössbauer spectroscopy, X-ray diffraction and
74 instrumental neutron activation analysis, in order to characterize the iron speciation, mineralogy and to
75 determine the concentration and distribution of 29 chemical elements. Results are compared with those
76 obtained for the corresponding whole samples (Marques et al., 2016).

77 The main objectives of this work are therefore: (1) the chemical characterization of the clay-size
78 fraction of the surficial layer of soils developed on sediments and phonolitic pyroclasts in Brava Island
79 (Cape Verde); (2) the iron distribution in mineralogical phases of the clay-size fraction of the soils; (3)
80 the assessment of the $\text{Fe}^{3+}/(\text{Fe}^{2+}+\text{Fe}^{3+})$ ratio; and (4) the establishment of the geochemical patterns and
81 the identification of chemical elements with high contents. Thus a better knowledge of soils used for
82 agriculture in Brava Island is a major motivation of this work, contributing for the identification of
83 potential risks to humans coupled with the need of the population of this island to produce food.

84

85 **2. Geological setting, climate and study area**

86 The Cape Verde archipelago is composed of 10 islands and several islets, and is located 600 to
87 900 km west of the African coast, on the southwestern part of the Cape Verde Rise (Fig. 2A).
88 Generally moderate, the climate of Cape Verde islands is characterized by stable temperatures with
89 extreme aridity. Precipitation levels are unpredictable, depending on how the intertropical convergence
90 zone (ITCZ) progresses and how much tropical moisture it carries. Years may pass with little or no
91 precipitation. Marine and fluvial erosion and mass wasting processes have contributed to the present
92 morphology of the Brava Island (Madeira et al., 2008). Field observations revealed the presence of an
93 older basement composed of a submarine volcanic sequence (nephelinitic/ankaramitic hyaloclastites
94 and pillow lavas) and an intrusive complex (alkaline-carbonatite) that is unconformably covered by
95 younger sub-aerial volcanic deposits (dominated by phonolitic magmatism); sediments include alluvial
96 and mass wasting deposits. These sequences allowed the definition of major volcano-stratigraphic
97 units – Lower Unit, Middle Unit, Upper Unit, and Sediments (Madeira et al., 2010).

98

99 **3. Materials and methods**

100 The soils of Cape Verde archipelago are mainly inceptisols and entisols on basaltic substrate
101 with low organic matter, mainly of volcanic origin, and shallow (circa 30 cm depth) with a low water
102 holding capacity (Madeira and Ricardo, 2013). Field work and sampling was performed in 2013 in
103 Brava Island (see Fig. 2B). Sampling of nine surficial layer of the soils (0-20 cm depth), hereafter
104 referred to as topsoils, was performed: six developed on sediments and three on phonolitic pyroclasts
105 (Upper Unit). A wide variety of vegetables (like sweet potato, beans, corn, cabbage, carrots, etc), and
106 fruits (banana, mango, papaya, etc) are cultivated in this island. The irrigation of crops is dependent of
107 rainfall regime, but nowadays the drip irrigation system has been implemented in Brava. The sample
108 reference, UTM coordinates, altitude, granulometry, color, and geological unit/parent rock according
109 to Madeira et al. (2010) are given for each soil (Table 1).

110 The clay-size fraction of each topsoil was obtained as follows: circa 100 g of the $\phi < 50 \mu\text{m}$
111 fraction resulting from wet sieving with deionized water (nylon mesh) was used to obtain the $\phi < 2 \mu\text{m}$
112 fraction by sedimentation according to Stokes' law (Moore and Reynolds, 1997) after dispersion with
113 sodium hexametaphosphate (1%).

114 The mineralogical composition of the clay-size fraction was determined by X-ray diffraction
115 (XRD) of oriented specimens on glass slides using a Philips diffractometer, Pro Analytical, with Cu
116 $K\alpha$ radiation at 40 kV and 35 mA within the $2^\circ - 30^\circ 2\theta$ range, with a step size of $1^\circ 2\theta/\text{min}$. The
117 following treatments were performed: air drying, ethylene glycol solvation (EG), and heating (550
118 $^\circ\text{C}$). The minerals identification was done according to Brindley and Brown (1980), Moore and
119 Reynolds (1997), Thorez (1976) and Trindade et al. (2011).

120 Chemical elements concentrations were determined by instrumental neutron activation analysis
121 (INAA). Two reference materials were used in the evaluation of elemental concentrations by INAA:
122 soil GSS-4 and sediment GSD-9 from the Institute of Geophysical and Geochemical Prospecting
123 (IGGE). Reference values were taken from data tabulated by Govindaraju (1994). The samples and
124 standards were prepared for analysis by weighing 200–300 mg of powder into cleaned high-density
125 polyethylene vials. Two aliquots of each standard were used for internal calibration, and standard
126 checks were performed (QA/QC). Short and long irradiations were performed in the core grid of the
127 Portuguese Research Reactor (CTN/IST, at Bobadela) (Fernandes et al., 2010) at a thermal flux of
128 $3.96 \times 10^{12} \text{ n cm}^{-2} \text{ s}^{-1}$; $\phi_{\text{th}}/\phi_{\text{epi}} = 96.8$; $\phi_{\text{th}}/\phi_{\text{fast}} = 29.8$. Two γ -ray spectrometers were used. Corrections
129 for the spectral interference from U fission products in the determination of Ba, REE and Zr were
130 made according to Gouveia et al. (1987) and Martinho et al. (1991), and more details of the analytical
131 method may be found in Marques et al. (2011) and Prudêncio et al. (2006, 2015). Relative precision
132 and accuracy are, in general, to within 5%, and occasionally within 10%.

133 The ^{57}Fe Mössbauer measurements were recorded at 295 and 4 K in transmission mode using a
134 conventional constant acceleration spectrometer and a 25-mCi ^{57}Co source in Rh matrix. The velocity
135 scale was calibrated using an α -Fe foil at room temperature. Isomer shift values, IS, are given relative
136 to this standard. Powdered samples were packed together with lucite powder into perspex holders, in
137 order to obtain homogeneous and isotropic Mössbauer absorbers containing about 5 mg/cm^2 of natural
138 iron. The measurements taken at 4 K were obtained with the samples immersed in liquid He in a bath
139 cryostat. The spectra were fitted to Lorentzian lines using a non-linear least-squares method
140 (Waerenborgh et al., 1990).

141

142 4. Results

143 The XRD results for the clay-size fraction of topsoils from Brava Island (Cape Verde) showed
144 the existence of a significant vitreous component, evidenced by a bulge in the baseline of the
145 diffractograms and a low proportion of clay minerals crystalline phases. The clay minerals identified
146 in topsoils developed on sediments and phonolitic pyroclasts are:

147 - Sediments – illite, kaolin minerals and traces of chlorite and mixed-layer illite/smectite (I/Sm)
148 in all samples; in addition smectite was also identified in the topsoils developed on a slope talus (7-
149 BRV) and on a landslide deposit (8-BRV), both located on the western part of the island with
150 contributions from the Lower Unit and the Upper Unit (see Fig. 2B).

151 - Phonolitic pyroclasts – illite associated to traces of kaolin minerals, mixed-layer I/Sm and
152 chlorite.

153 The chemical results obtained by INAA for the clay-size fraction of the topsoils are given in
154 Table 2. Significant variations were found for the studied chemical elements (in increasing order): $c <$
155 30% for Fe, Ga, Cr, Rb, W and Cs; $30\% \leq c \leq 50\%$ for As, K, Mn, U, Ta, Zn, Br, Sc, Lu, Yb, Th and
156 Co; $c > 50\%$ for Tb, Ba, Zr, Sm, Na, Eu, Hf, Ce, Nd, La and Sb. Arsenic, U and particularly Zn
157 concentrations may differentiate soils developed on sediments and on phonolitic pyroclasts, being
158 lower on sediments, even on soil 2-BRV which corresponds to an alluvium with a major contribution
159 from the Upper Unit.

160 Mössbauer spectra (Fig. 3) of all the samples taken at room temperature consist of one doublet.
161 The estimated parameters for these doublets, summarized in Table 3, are typical of Fe^{3+} (Greenwood
162 and Gibb, 1971). At 4 K all the spectra (Fig. 4) show in addition to the doublet six broad absorption
163 peaks which were analyzed by two magnetic sextets.

164

165 4.1. Rare earth elements patterns

166 The rare earth elements (REE) patterns of the clay-size fraction of topsoils developed on
167 sediments and on phonolitic pyroclasts relative to chondrites, and to the corresponding whole sample
168 (data from Marques et al., 2016) are shown in Fig. 5A and 5B, respectively.

169 - Sediments - the lowest REE contents, fractionation between light REE (LREE) and heavy
170 REE (HREE) ($(La/Yb)_{ch} = 15$), and a positive Ce anomaly ($Ce/Ce^* = 1.2$) were found in topsoils 7-
171 BRV and 8-BRV, located in the western part of the island with contributions from the Lower Unit and
172 the Upper Unit (Fig. 5A); in the alluvium deposits located in the plateau with a major contribution
173 from the Upper Unit (samples 2-BRV and 32-BRV) similar REE contents and patterns were found,
174 except for higher LREE contents, particularly La, originating a higher LREE/HREE ratio ($(La/Yb)_{ch} =$
175 35) in the sample 32-BRV, located close to the Minhoto Fault Zone (MFZ); the highest REE contents
176 were found in alluvium deposits (28-BRV and 29-BRV) in the southern part of the island with
177 contributions from the Middle and the Upper Unit. A negative Ce anomaly also occurs ($Ce/Ce^* = 0.7$).
178 Comparing the REE in the clay-size fraction with the respective whole sample (Fig. 5B), the LREE
179 and HREE are in general more enriched than the middle REE (MREE). A positive Ce anomaly occurs,
180 particularly in the topsoils developed on sediments of the western part the island (7-BRV, 8-BRV) and
181 in the alluvium deposit of the bottom of a crater in the southern part of the plateau (2-BRV).

182 - Phonolitic pyroclasts – REE patterns relative to chondrites (Fig. 5C) show a slight negative Ce
183 anomaly ($Ce/Ce^* = 0.6-0.8$). The sample collected near the MFZ has the highest REE contents and
184 fractionation ($(La/Yb)_{ch} = 71$). The remaining topsoils present similar contents and patterns. When
185 compared to the respective whole sample (Fig. 5D), the two topsoils located near the MFZ (18-BRV
186 and 31-BRV) show a similar pattern with a negative Ce anomaly.

187

188 4.2. Other chemical elements

189 The distribution patterns of the other chemical elements in the clay-size fraction relative to the
190 corresponding whole sample are shown in Fig. 6.

191 - Sediments – a general depletion of Fe and Cr is observed; Na and K are also depleted except in
192 sample 7-BRV (talus deposit). An enrichment of Mn, As, Br, Sb, W and Th occurs in the clay-size
193 fraction of all studied topsoils; the same tendency is observed for Zn, except in sample 2-BRV
194 (alluvium in the bottom of a crater). The topsoils developed on the sediments located in the southern
195 part of the island (28-BRV and 29-BRV) with major contributions from the Middle and Upper Unit,

196 can be distinguished by the highest depletion of Fe, Ga, Rb, Zr, Hf, Ta, and U in the clay-size fraction
197 (Fig. 6A).

198 - Phonolitic pyroclasts – Fe, Cr, Rb, and Ba are depleted in the clay-size fraction of the three
199 topsoils studied; Zn, As, Br, Sb and Th are enriched (Fig. 6B). Arsenic, Br and particularly Sb can be
200 strongly enriched (up to 70 times) in the clay-size of topsoils developed on both sediments and
201 phonolitic pyroclasts.

202

203 5. Discussion

204 The doublet and sextets observed in Mössbauer spectra at 4 K of the clay-size fraction of Brava
205 Island soils correspond to contributions from different Fe-bearing phases, as explained in detail in
206 Marques et al. (2014b) the doublet may be assigned to Fe^{3+} in the silicate phases and the sextets to Fe^{3+}
207 oxides (Murad, 1998). All these oxides are nano-sized since at room temperature no sextets are
208 observed. The poor crystallinity (small crystal size, unspecific particle shape, structural disorder) and
209 Fe^{3+} isomorphous substitution by impurity cations such as Al^{3+} give rise to a range of isomer shifts,
210 quadrupole interactions and magnetic hyperfine fields (Murad, 1998; Vandenberghe et al., 2000). This
211 range of parameter values may explain the significant peak broadening that prevents the clear
212 identification of resolved contributions from different oxides, namely hematite or maghemite which
213 were detected in the whole fraction of these samples (Marques et al., 2016). In summary, Mössbauer
214 spectroscopy shows that in the clay-size fraction of the studied topsoils all the Fe is present as Fe^{3+} and
215 all the Fe oxides are nano-sized independently of the topsoils weathering degree deduced from the
216 analysis of the whole samples (Marques et al., 2016).

217 As far as REE are concerned, the relative Ce enrichment observed in the clay-size fraction of
218 some of the studied sediments (2-BRV, 7-BRV and 8-BRV) indicates stronger oxidizing conditions
219 leading to $\text{Ce}^{3+} \rightarrow \text{Ce}^{4+}$ with preferred retention of this element on the clay-size particles when
220 compared to the other LREE. Sample 2-BRV also has the highest fraction of Fe in nano-sized oxides
221 (Table 3). This is consistent with the Ce behavior, assuming that nano-sized Fe oxides may be the Fe-
222 containing end-products of weathering. A negative Ce anomaly is observed in the alluvium sediments
223 located in the south of the island with contributions from the Middle Unit and the Upper Unit, mainly

224 due to high La contents in the fine particles (28-BRV, 29-BRV). In these samples a negative Eu
225 anomaly is also observed suggesting the preferential presence of this element in the coarser particles
226 (see Fig. 5B).

227 Thus, REE contents and patterns in the clay-size fraction of all studied samples appear to
228 depend on the composition of the parent rock of the topsoils. Regardless of the general enrichment of
229 the REE in the clay-size fraction found both in sediments and phonolitic pyroclasts, significant
230 differences occur in the concentrations and distribution relative to the corresponding whole sample,
231 which may reflect distinct oxidizing conditions as the Ce anomaly suggests; eventual contributions of
232 fine particles resulting from volcanic activities, particularly close to MFZ that crosses the island in a
233 NE-SW direction, may also play an important role.

234 Among the other chemical elements determined in the clay-size fraction of soils, the depletion
235 of Fe and Cr on sediments suggest their occurrence as iron oxides and ferromagnesian minerals
236 present in coarser particles. When the whole samples of both sediments and phonolitic pyroclasts of
237 Brava Island were studied (Marques et al., 2016) a correlation was found between the concentration of
238 As, Br and Sb and the oxidation degree of Fe. The present data, showing that these elements are
239 enriched in the clay-size fraction where all the Fe oxides are nano-sized, confirms the predominant
240 adsorption of As, Br and Sb on these nano-particles surface. Despite the general low contents of these
241 trace elements, their presence in fine particles of soils from Brava Island consisting of poorly
242 crystallized clay and oxide phases as well as vitreous phases may contribute for their mobility and
243 accumulation in plants, and in groundwater. Also dust deposition onto the plant leaves should be
244 considered as potential risks to the local population using these soils for agriculture to produce food.
245 All the Fe²⁺ detected in the whole samples of topsoils (Marques et al., 2016), most of it within the
246 silicate structures, is present in the coarser fraction of the samples since no Fe²⁺ is detected in the clay-
247 size fraction. This may be related to the lower Fe content of the clay-size fraction when compared to
248 the whole sample. Sediment samples 28-BRV and 29-BRV have very similar Fe speciation and
249 chemical composition both when analyzed as whole samples (Marques et al., 2016) and as clay-sized
250 fraction. All the other soils which have similar chemical compositions have significantly different
251 fractions of Fe in nano-oxides (for instance 2-BRV and 32-BRV, or 31-BRV and 40-BRV).

252 Considering the geographical proximity of 28-BRV and 29-BRV they seem to be soils developed on
253 the same sedimentary formation in similar conditions during the depositional event, and to have
254 suffered similar weathering processes during the same time span.

255

256 **6. Conclusions**

257 The elemental distribution in the clay-size fraction of the surficial layer of soils developed on
258 sediments and on phonolitic pyroclasts in Brava Island (Cape Verde) show significant chemical
259 content variations, particularly for Fe, Ga, Cr, Rb, W and Cs. A general enrichment of REE in the
260 clay-size fraction relative to the whole sample is observed in both soils developed on sediments and
261 phonolitic pyroclasts. Nevertheless, significant differences are found in REE concentration and
262 distribution which may be partially due to weathering, since different oxidizing conditions are
263 suggested by the Ce anomalies. Iron and chromium are depleted. All the iron in the clay-size fraction
264 of the topsoils is present as Fe³⁺ pointing to oxidation as the main chemical weathering mechanism.
265 The iron oxides in the clay-size fraction are nano-sized. Among the chemical elements studied, the
266 most enriched in the clay-size fraction are As, Br and especially Sb. Considering the positive
267 correlation found for the whole samples between the iron oxidation degree and the concentration of
268 these elements (Marques et al., 2016) they are most likely adsorbed onto the Fe oxides nano-particles
269 surface as well as in poorly crystalline clay minerals. In spite of the low contents of As, Br and Sb
270 their presence on nano-sized particles and in a significant vitreous component in the clay-size fraction
271 of these soils contributes for their mobility and distribution in the biogeochemical cycles having a
272 potential impact on the agriculture in Brava Island.

273

274 **References**

- 275 Anders, E., Grevesse, N., 1989. Abundances of the elements: meteoritic and solar. *Geochimica et*
276 *Cosmochimica Acta* 53, 197–214. [https://doi.org/10.1016/0016-7037\(89\)90286-X](https://doi.org/10.1016/0016-7037(89)90286-X)
- 277 Brindley, G.W., Brown, G., 1980. *Crystal Structures of Clay Minerals and their X-ray Identification*.
278 Monograph 5, Mineralogical Society, London.

- 279 Cronin, S.J., Neall, V.E., Lecointre, J.A., Hedley, M.J., Loganathan, P., 2003. Environmental hazards
280 of fluoride in volcanic ash: a case study from Ruapehu volcano, New Zealand. *Journal of Volcanology
281 and Geothermal Research* 121, 271–291. [https://doi.org/10.1016/S0377-0273\(02\)00465-1](https://doi.org/10.1016/S0377-0273(02)00465-1)
- 282 Fernandes, A.C., Santos, J.P., Marques, J.G., Kling, A., Ramos, A.R., Barradas, N.P., 2010. Validation
283 of the Monte Carlo model supporting core conversion of the Portuguese Research Reactor (RPI) for
284 neutron fluence rate determinations. *Annals of Nuclear Energy* 37, 1139-1145.
285 <https://doi.org/10.1016/j.anucene.2010.05.004>
- 286 Frogner, P., Gíslason, S.R., Óskarsson, N., 2001. Fertilizing potential of volcanic ash in ocean surface
287 water. *Geology* 29, 487–490. <http://dx.doi.org/10.1130/0091-7613>
- 288 Gouveia, M.A., Prudêncio, M.I., Freitas, M.C., Martinho, E., Cabral, J.M.P., 1987. Interference from
289 uranium fission products in the determination of rare earths, zirconium and ruthenium by instrumental
290 neutron activation analysis in rocks and minerals. *Journal of Radioanalytical and Nuclear Chemistry* 2
291 (Articles 14), 309-318. <http://dx.doi.org/10.1007/BF02039805>
- 292 Greenwood, N.N., Gibb, T.C., 1971. *Mössbauer Spectroscopy*, Chapman and Hall, Ltd. Publishers,
293 London.
- 294 Govindaraju, K., 1994. Compilation of working values and sample description for 383 geostandards.
295 *Geostandards Newsletter* 18, 1–158. <http://dx.doi.org/10.1046/j.1365-2494.1998.53202081.x-i1>
- 296 Han, F.X., 2007. *Biogeochemistry of Trace Elements in Arid Environments*. Springer Netherlands,
297 ISBN978-1-4020-6024-3, 368p.
- 298 Jones, M.T., Gíslason, S.R., 2008. Rapid releases of metal salts and nutrients following the deposition
299 of volcanic ash into aqueous environments. *Geochimica et Cosmochimica Acta* 72, 3661–3680.
300 <https://doi.org/10.1016/j.gca.2008.05.030>
- 301 Korotev, R.L., 1996a. A self-consistent compilation of elemental concentration data for 93
302 geochemical reference samples. *Geostandards and Geoanalytical Research* 20, 217–245.
303 <https://doi.org/10.1111/j.1751-908X.1996.tb00185.x>
- 304 Korotev, R.L., 1996b. On the relationship between the Apollo 16 ancient regolith breccias and
305 feldspathic fragmental breccias, and the composition of the prebasin crust in the central highlands of

- 306 the moon. *Meteoritics and Planetary Science* 31, 403–412. <https://doi.org/10.1111/j.1945->
307 [5100.1996.tb02078.x](https://doi.org/10.1111/j.1945-5100.1996.tb02078.x)
- 308 Madeira, J., Brum da Silveira, A., Mata, J., Mourão, C., Martins, S., 2008. The role of mass
309 movements on the geomorphologic evolution of ocean islands: examples from Fogo and Brava in the
310 Cape Verde archipelago. *Comunicações Geológicas* 95, 99–112.
- 311 Madeira, J., Mata, J., Mourão, C., Brum da Silveira, A., Martins, S., Ramalho, R., Hoffmann, D.L.,
312 2010. Volcano-stratigraphic and structural evolution of Brava Island (Cape Verde) based on
313 $^{40}\text{Ar}/^{39}\text{Ar}$, U-Th and field constraints. *Journal of Volcanology and Geothermal Research* 196, 219–
314 235. <https://doi.org/10.1016/j.jvolgeores.2010.07.010>
- 315 Madeira, M., Ricardo, P., 2013. Os solos de Cabo Verde. Seu enquadramento no sistema de referência
316 mundial de solos. *Revista de Ciências Agrárias* 36 (4), 377–392.
- 317 Marques, R., Prudêncio, M.I., Dias, M.I., Rocha, F., 2011. Patterns of rare earth and other trace
318 elements in different size fractions of clays of Campanian-Maastrichtian deposits from the Portuguese
319 western margin (Aveiro and Taveiro Formations). *Chemie der Erde/Geochemistry* 71, 337–347.
320 <http://dx.doi.org/10.1016/j.chemer.2011.02.002>
- 321 Marques, R., Prudêncio, M.I., Rocha, F., Cabral Pinto, M.S., Silva, M.M.V.G., Ferreira da Silva, E.,
322 2012. REE and other trace and major elements in the topsoil layer of Santiago Island, Cape Verde.
323 *Journal of African Earth Sciences* 64, 20–33. <http://dx.doi.org/10.1016/j.jafrearsci.2011.11.011>
- 324 Marques, R., Prudêncio, M.I., Waerenborgh, J.C., Rocha, F., Dias, M.I., Ruiz, F., Ferreira da Silva, E.,
325 Abad, M., Muñoz, A.M., 2014a. Origin of reddening in a paleosol buried by lava flows in Fogo Island
326 (Cape Verde). *Journal of African Earth Sciences* 96, 60–70,
327 <http://dx.doi.org/10.1016/j.jafrearsci.2014.03.019>
- 328 Marques, R., Waerenborgh, J.C., Prudêncio, M.I., Dias, M.I., Rocha, F., Ferreira da Silva, E., 2014b.
329 Iron speciation in volcanic topsoils from Fogo Island (Cape Verde) - iron oxide nanoparticles and
330 trace elements concentrations. *Catena* 113, 95–106. <http://dx.doi.org/10.1016/j.catena.2013.09.010>
- 331 Marques, R., Prudêncio, M.I., Waerenborgh, J.C., Rocha, F., Ferreira da Silva, E., Dias, M.I., Madeira,
332 J., Vieira, B.J.C., Marques, J.G., 2016. Geochemical fingerprints in topsoils of the volcanic Brava
333 island, Cape Verde. *Catena* 147, 522–535. <http://dx.doi.org/10.1016/j.catena.2016.08.008>

- 334 Marques, R., Prudêncio, M.I., Waerenborgh, J.C., Vieira, B.J., Rocha, F., Dias, M.I., Madeira, J.,
335 Mata, J., 2017a. Extrusive carbonatite outcrops - a source of chemical elements imbalance in topsoils
336 of oceanic volcanic islands. *Catena* 157, 333-343. <http://dx.doi.org/10.1016/j.catena.2017.05.035>
- 337 Marques, R., Prudêncio, M.I., Freitas, M.C., Dias, M.I., Rocha, F., 2017b. Chemical element
338 accumulation in tree bark grown in volcanic soils of Cape Verde – a first biomonitoring of Fogo
339 Island. *Environmental Science and Pollution Research*, 24, 11978-11990.
340 <http://dx.doi.org/10.1007/s11356-015-5498-z>
- 341 Marques, R., Prudêncio, M.I., Waerenborgh, J.C., Rocha, F., Ferreira da Silva, E., Dias, M.I., Vieira,
342 B.J.C., Marques, J.G., Franco, D., 2017c. Volcanic conduits of the Chã das Caldeiras caldera (Fogo
343 Island, Cape Verde) – REE and Fe crystalchemistry. *Procedia Earth and Planetary Science* 17, 928-
344 931. <http://dx.doi.org/10.1016/j.proeps.2017.01.023>
- 345 Martin, R.S., Mather, T.A., Pyle, D.M., Watt, S.F.L., Day, J.A., Collins, S.J., Wright, T.E., Aiuppa,
346 A., Calabrese, S., 2009. Sweet chestnut (*Castanea sativa*) leaves as a bio-indicator of volcanic gas,
347 aerosol and ash deposition onto the flanks of Mt Etna in 2005–2007. *Journal of Volcanology and*
348 *Geothermal Research* 179, 107–119. <https://doi.org/10.1016/j.jvolgeores.2008.10.012>
- 349 Martinho, E., Gouveia, M.A., Prudêncio, M.I., Reis, M.F., Cabral, J.M.P., 1991. Factor for correcting
350 the ruthenium interference in instrumental neutron activation analysis of barium in uraniferous
351 samples. *Applied Radiations and Isotopes* 42, 1067-1071. [https://doi.org/10.1016/0883-](https://doi.org/10.1016/0883-2889(91)90012-P)
352 [2889\(91\)90012-P](https://doi.org/10.1016/0883-2889(91)90012-P)
- 353 Moore, D.M., Reynolds, R.C., 1997. *X-ray Diffraction and the Identification and Analysis of Clay*
354 *Minerals*, second ed. Oxford University Press.
- 355 Munsell, Color, 1998. *Soil Color Charts*. Revised Washable Edition, New Windsor, NY.
- 356 Murad, E., 1998. Clays and clay minerals: What can Mössbauer spectroscopy do to help understand
357 them? *Hyperfine Interactions* 117, 39-70. <https://doi.org/10.1023/A:1012635124874>
- 358 Neall, V.E., 2007. Volcanic Soils, in *Land Use and Land Cover*, Honorary Theme Editor(s), in
359 *Encyclopedia of Life Support Systems (EOLSS)*, Developed under the Auspices of the UNESCO,
360 Eolss Publishers, Oxford, UK.

- 361 Nriagu, J.O., 1989. A global assessment of natural sources of atmospheric trace metals. *Nature* 338,
362 47-49. <http://dx.doi.org/10.1038/338047a0>
- 363 Prudêncio, M.I., Sequeira Braga, M.A., Oliveira, F., Dias, M.I., Delgado, M., Martins, M., 2006. Raw
364 material sources for the roman Bracaraense ceramic (NW Iberian Peninsula). *Clays and Clay Minerals*
365 54 (5), 639-651. <http://dx.doi.org/10.1346/CCMN.2006.0540510>
- 366 Prudêncio, M.I., Valente, T., Marques, R., Sequeira Braga, M.A., Pamplona, J., 2015. Geochemistry
367 of rare earth elements in a passive treatment system built for acid mine drainage remediation.
368 *Chemosphere* 138, 691-700. <http://dx.doi.org/10.1016/j.chemosphere.2015.07.064>
- 369 Thorez, J., 1976. *Practical Identification of Clay Minerals*. G. Lelotte, Dison, Belgium.
- 370 Trindade, M.J., Dias, M.I., Rocha, F., Prudêncio, M.I., Coroado, J., 2011. Bromine volatilization
371 during firing of calcareous and non-calcareous clays: Archaeometric implications. *Applied Clay*
372 *Science* 53, 489-499. <https://doi.org/10.1016/j.clay.2010.07.001>
- 373 Vandenberghe, R.E., Barrero, C.A., da Costa, G.M., Van San, E., De Grave, E., 2000. Mössbauer
374 characterization of iron oxides and (oxy)hydroxides: the present state of the art. *Hyperfine Interactions*
375 126, 247-259. <http://dx.doi.org/10.1023/A:1012603603203>
- 376 Waerenborgh, J.C., Annersten, H., Ericsson, T., Figueiredo, M.O., Cabral, J.M.P., 1990. A Mössbauer
377 study of natural gahnite spinels showing strongly temperature dependent quadrupole splitting
378 distributions. *European Journal of Mineralogy* 2, 267-271. <http://dx.doi.org/10.1127/ejm/2/3/0267>
- 379 Watt, S.F.L., Pyle, D.M., Mather, T.A., Martin, R.S., Matthews, N.E., 2009. Fallout and distribution of
380 volcanic ash over Argentina following the May 2008 explosive eruption of Chaitén, Chile. *Journal of*
381 *Geophysical Research Solid Earth* 114, B04207. <http://dx.doi.org/10.1029/2008JB006219>

382

383 **Acknowledgments**

384 Grateful acknowledgments are made to the Laboratory of Nuclear Engineering (LEN) and also to the
385 staff of the Portuguese Research Reactor (RPI) of CTN/IST for their assistance with the neutron
386 irradiations.

387

388 **Funding information**

389 Research funded by Fundação para a Ciência e a Tecnologia (FCT, Portugal) through the projects
390 UID/GEO/04035/2013 and UID/Multi/04349/2013.

391

392 Figure Captions

393 Fig. 1. Photographs of Brava Island (Cape Verde) with a view to agriculture soils developed on (A)
394 phonolitic pyroclasts (Nova Sintra), and (B) terrace sediments (Tantum).

395 Fig. 2. A) Location of Brava Island in the Cape Verde archipelago, and B) Sampling location of nine
396 studied topsoils of the Brava Island (superposed to the Brava geological map by Madeira et al.
397 (2010)).

398 Fig. 3. Mössbauer spectra taken at 295 K of the clay-size fraction of three topsoils. The lines over the
399 experimental points are doublets corresponding to Fe^{3+} . The estimated parameters for these doublets,
400 shown slightly shifted for clarity, are collected in Table 2.

401 Fig. 4. Mössbauer spectra taken at 4 K of the clay-size fraction of topsoils from Brava Island (Cape
402 Verde): A) five topsoils developed on sediments; and B) three topsoils developed on phonolitic
403 pyroclasts. The lines over the experimental points are the sum of a doublet and two sextets
404 corresponding to Fe^{3+} in silicates and nano-sized oxides, respectively. The estimated parameters for
405 these doublet and sextets, shown slightly shifted for clarity, are collected in Table 2.

406 Fig. 5. REE patterns of the clay-size fraction of topsoils from Brava Island relative to chondrites
407 (values of Anders and Grevesse (1989) multiplied by 1.36 according Korotev (1996a, 1996b)) and to
408 the respective whole samples: A) and B) soils developed on sediments; and C) and D) soils developed
409 on phonolitic pyroclasts.

410 Fig. 6. Trace element distribution in the clay-size fraction relative to the respective whole sample of
411 soils from Brava Island: A) developed on sediments and B) developed on phonolitic pyroclasts.

412

413 Table Captions

414 Table 1. Geological unit/parent rock, sample references, UTM coordinates (m), altitude (m),
415 granulometry and color of topsoils from Brava Island (Cape Verde).

- 416 Table 2. Sample references, and chemical composition of the clay-size fraction of topsoils from Brava
417 Island (Cape Verde).
- 418 Table 3. Estimated parameters from the Mössbauer spectra, taken at different temperatures, of the
419 clay-size fraction of Brava Island topsoil samples.

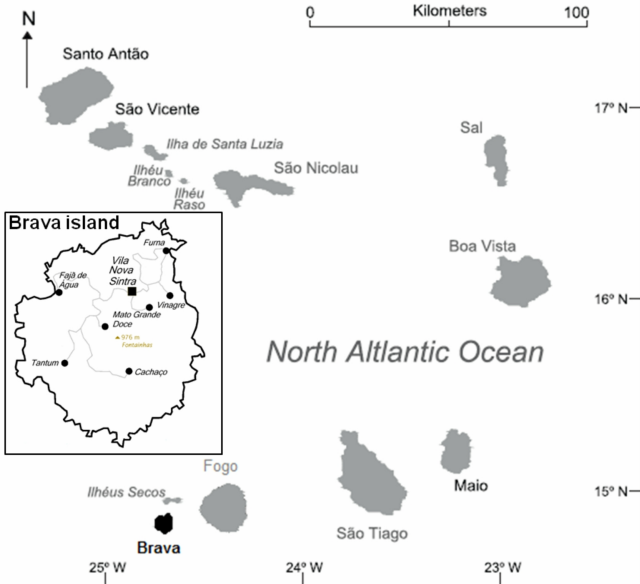
ACCEPTED MANUSCRIPT

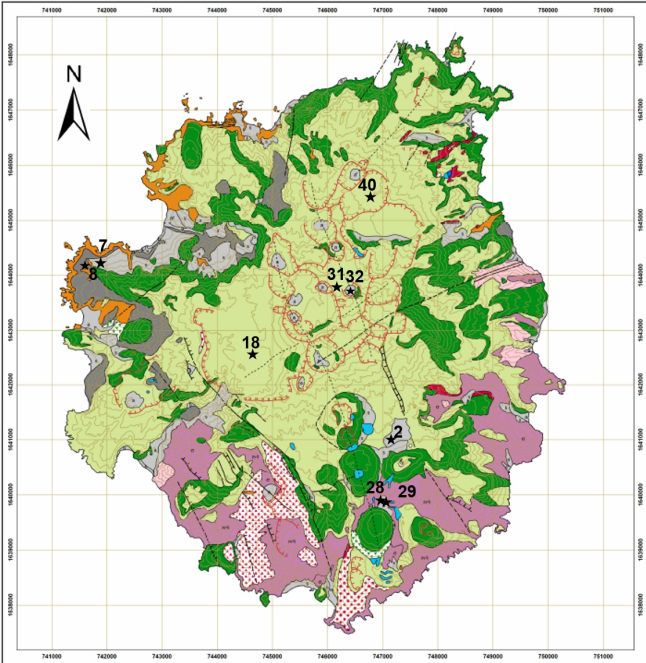
Highlights

- REE enrichment in the clay-size fraction of sediments and phonolitic pyroclast soils
- High concentrations of As, Br and especially Sb in clay-size fraction
- Predominant adsorption of As, Br and Sb on nano-sized iron oxide particles surfaces
- Only Fe(III) occurs in clay-size fraction of the topsoils
- All the Fe oxides occurring in the fine fractions are nano-sized







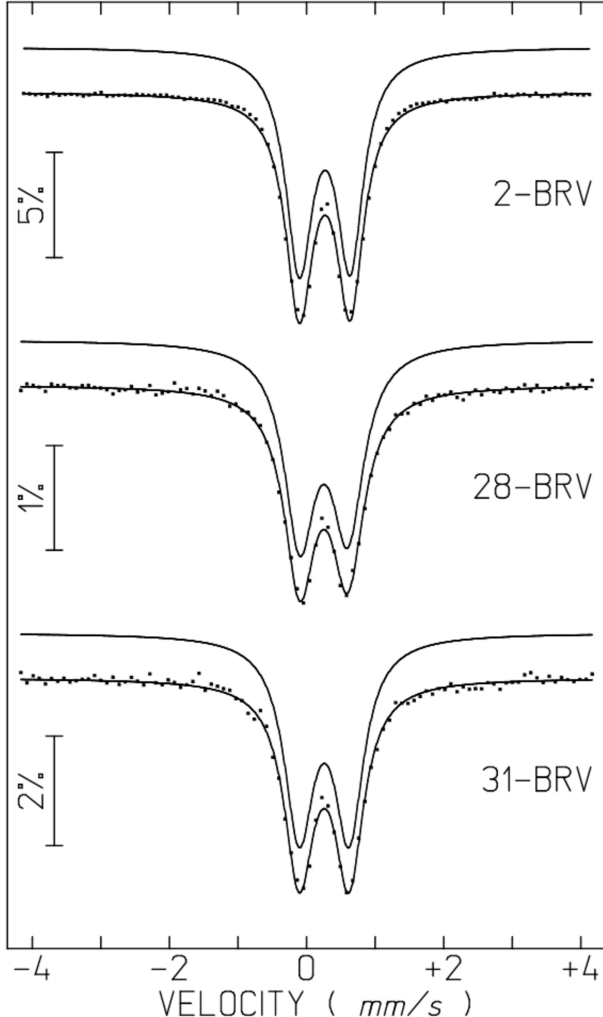


1:25 000 Scale



Contour interval of 50 meters

RELATIVE TRANSMISSION



2-BRV

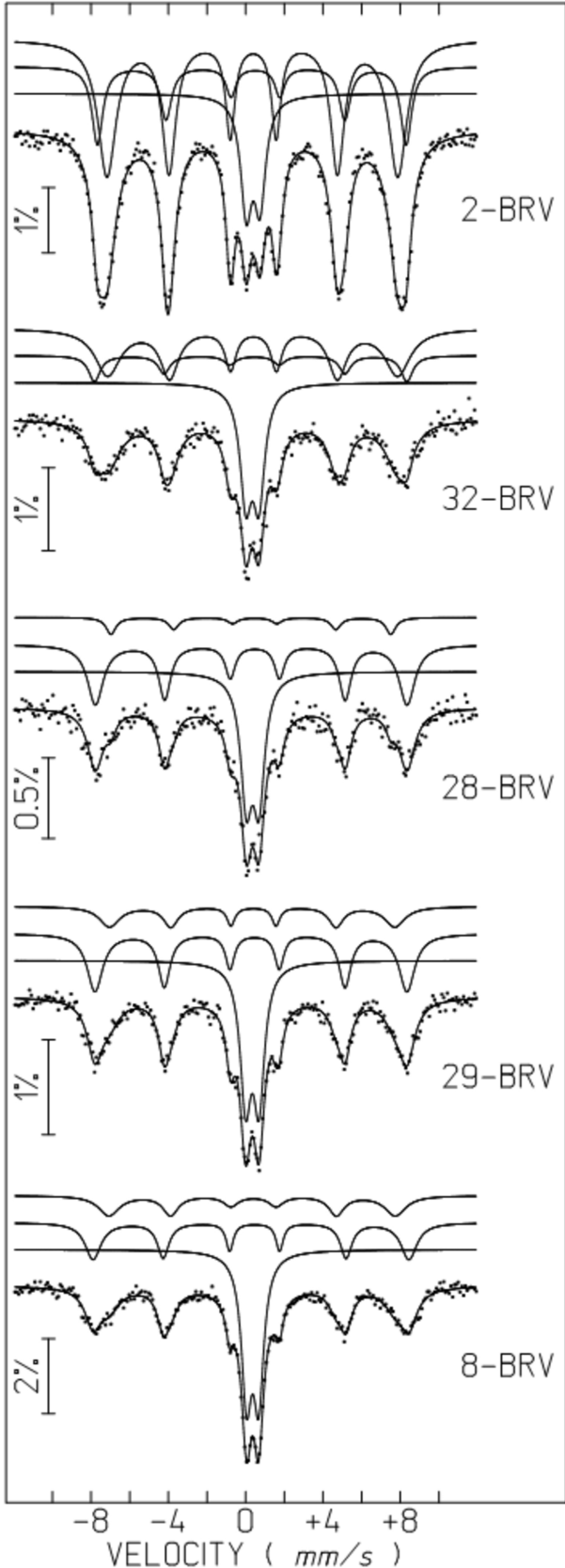
28-BRV

31-BRV

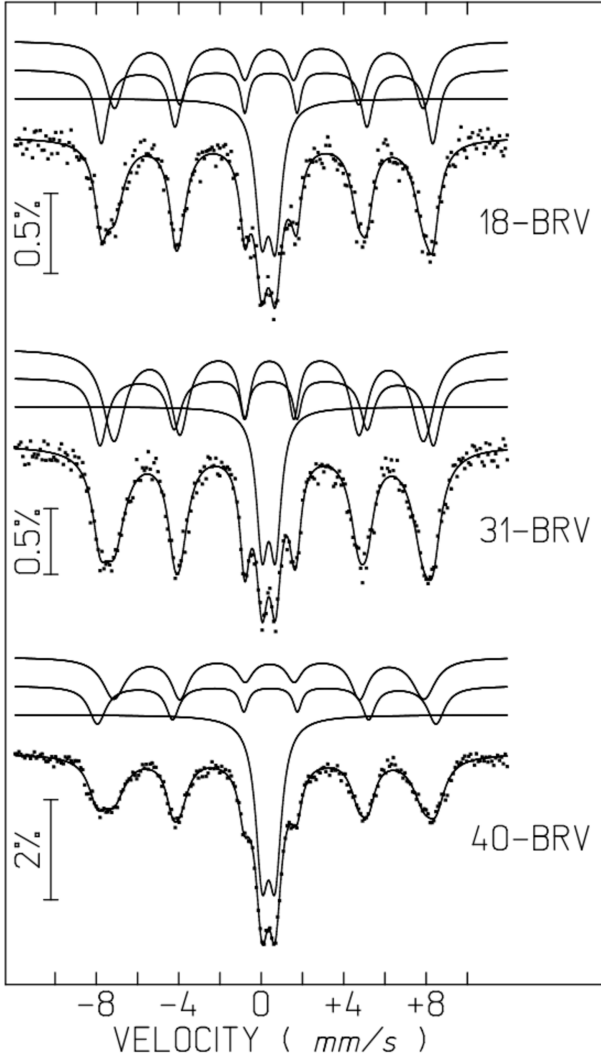
-4 -2 0 +2 +4

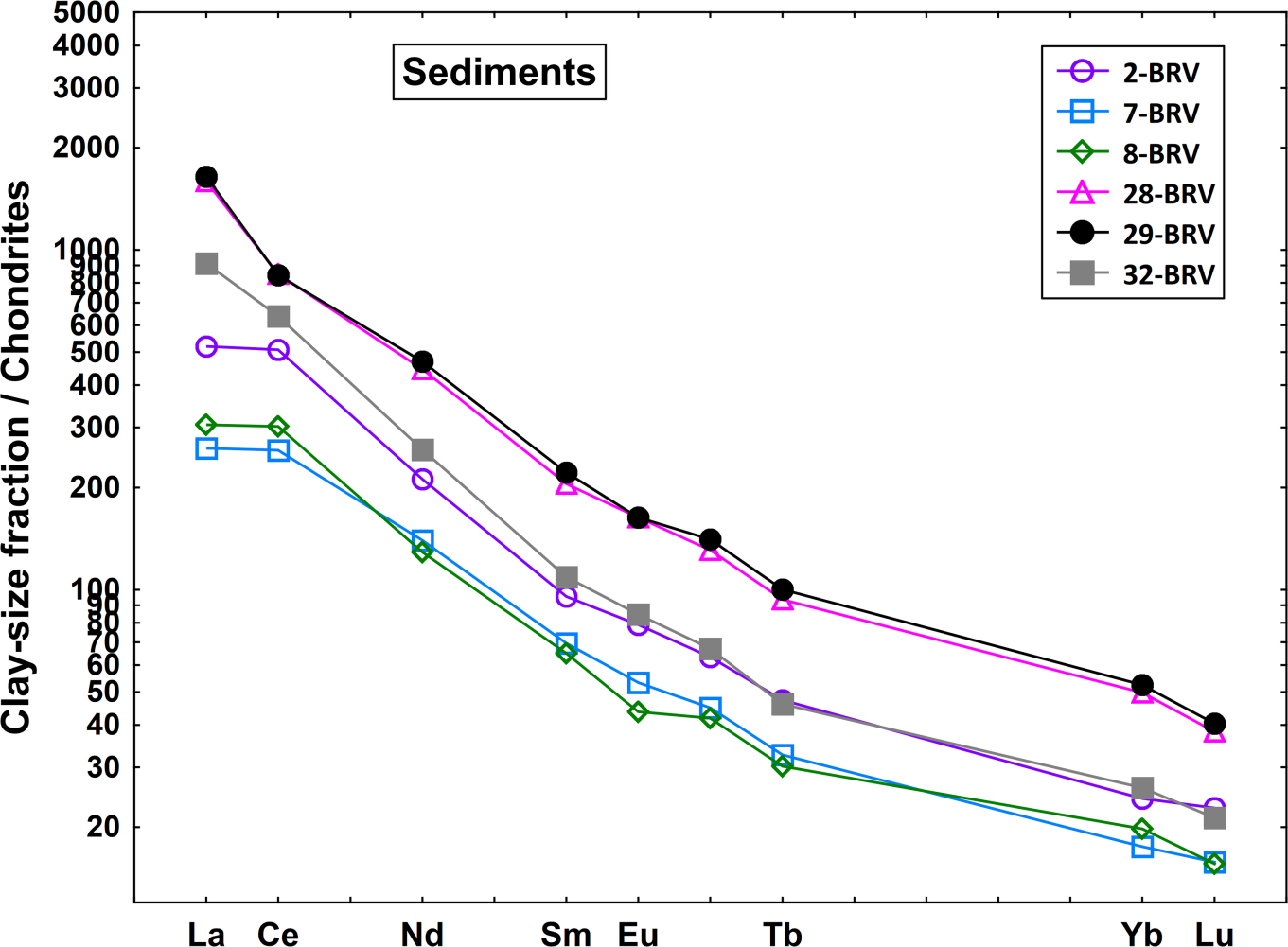
VELOCITY (*mm/s*)

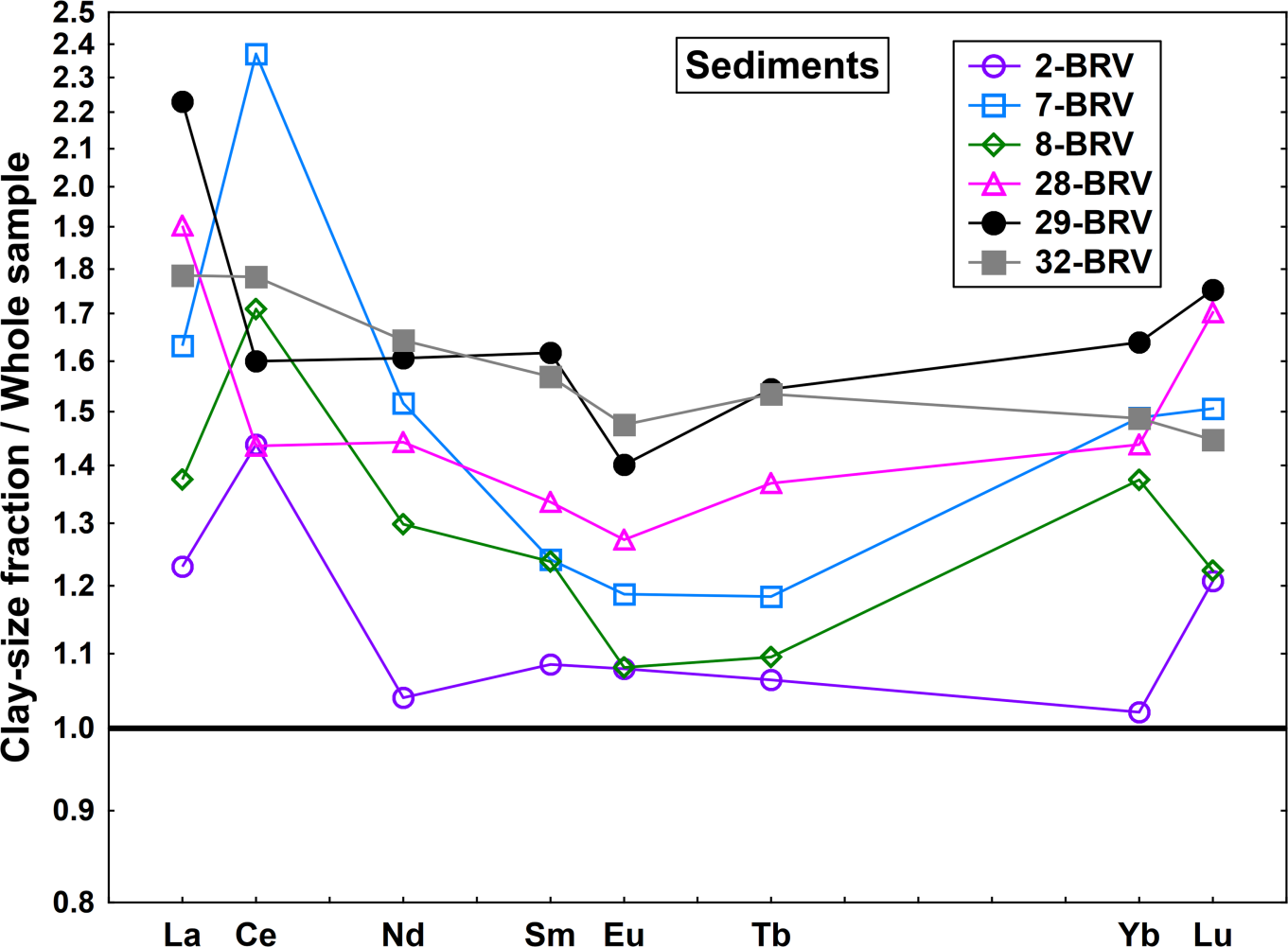
RELATIVE TRANSMISSION

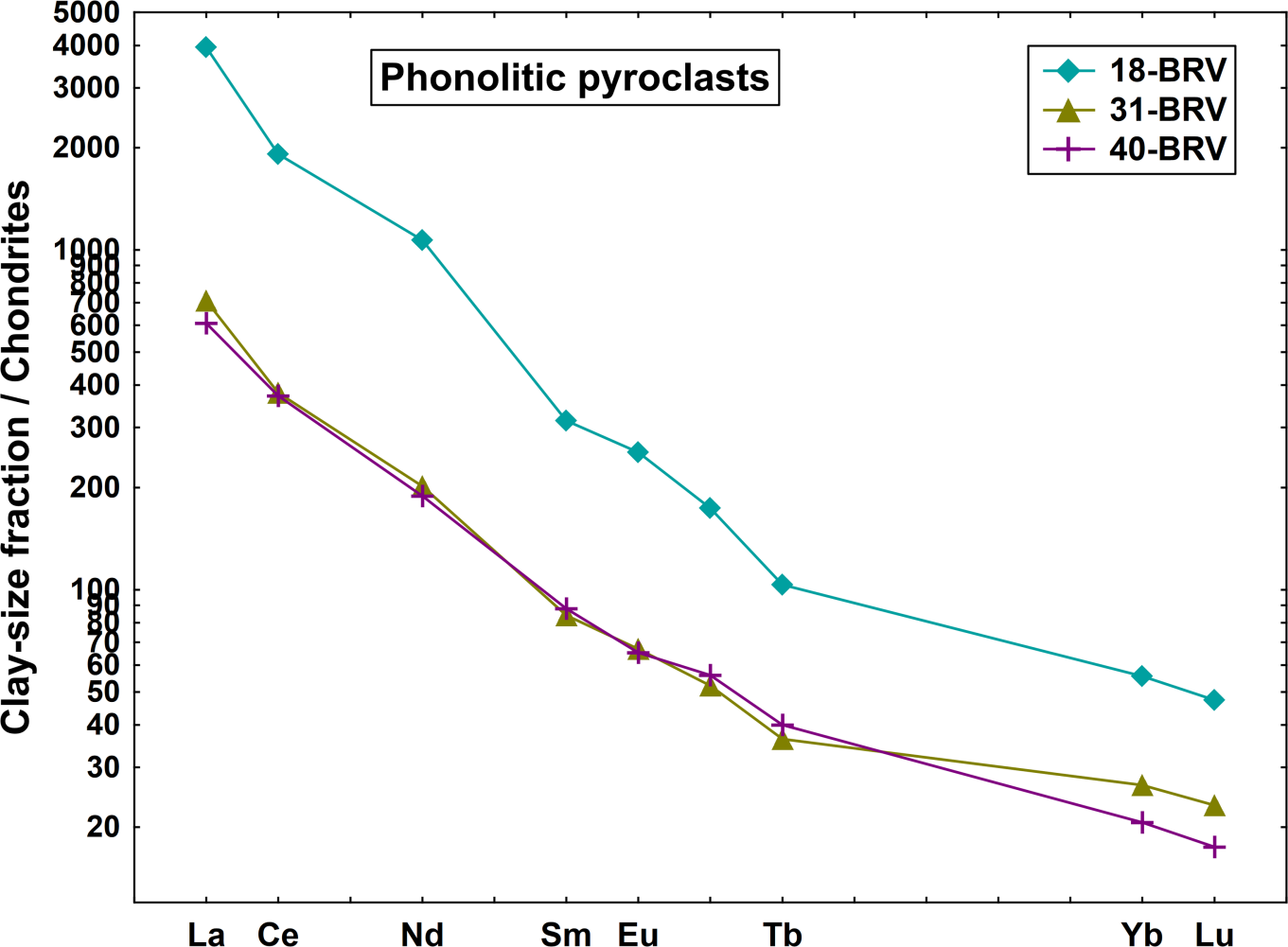


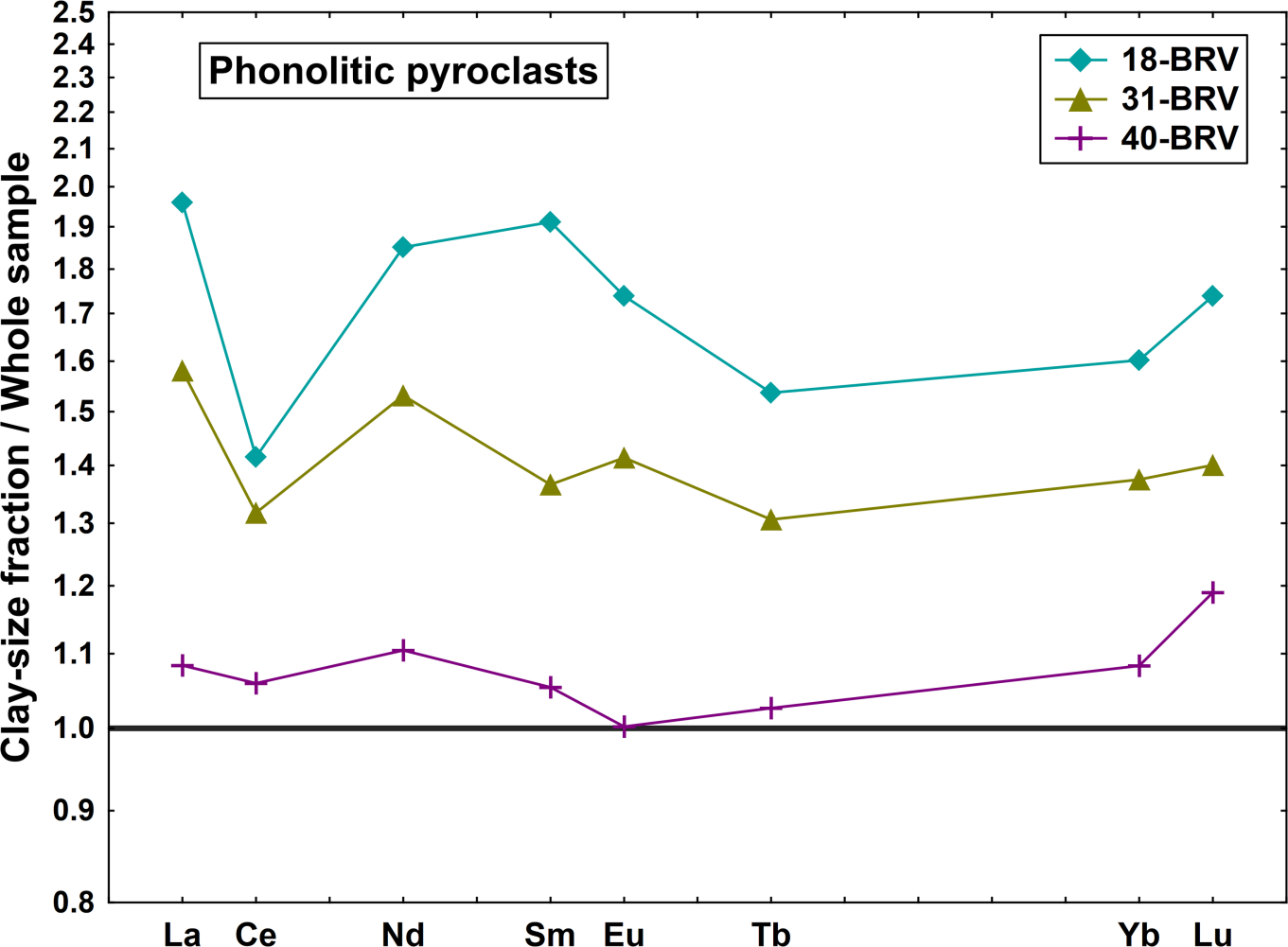
RELATIVE TRANSMISSION

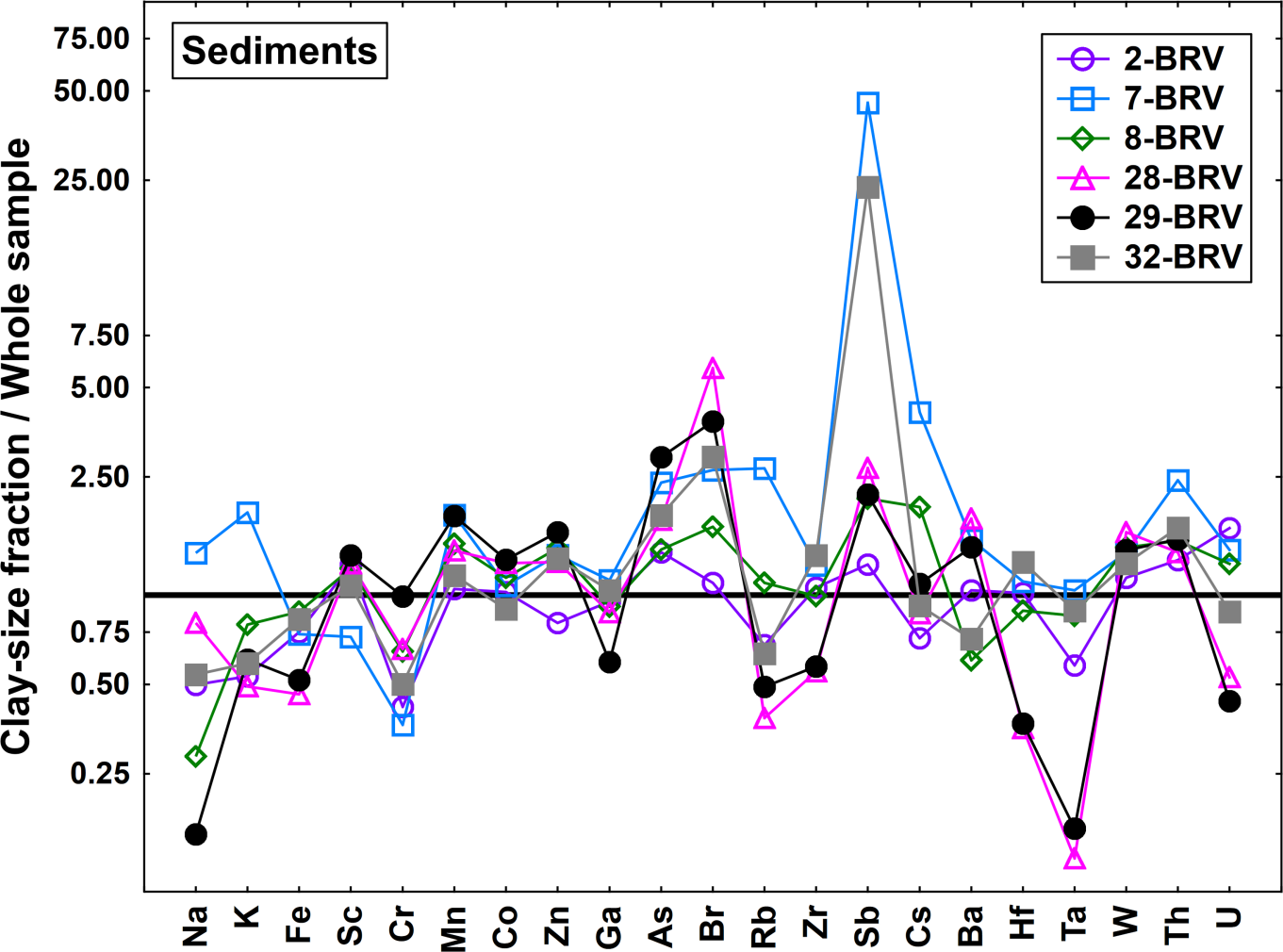












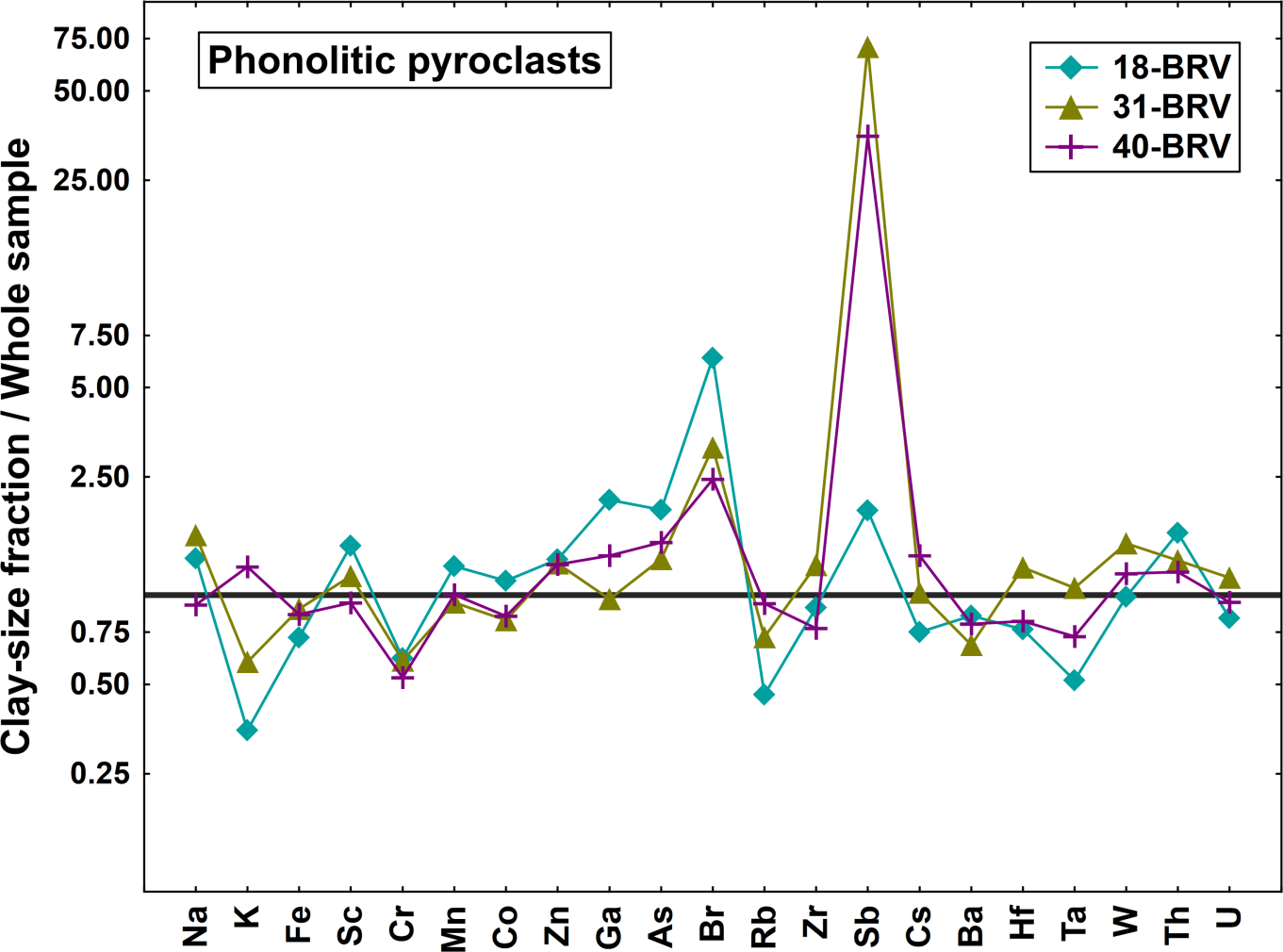


Table 1. Geological unit/parent rock, sample references, UTM coordinates (m), altitude (m), granulometry and color of topsoils from Brava Island (Cape Verde).

Geological Unit	Sediments					Upper Unit			
	Parent rock	Alluvium	Slope talus	Landslide deposits	Alluvium	Alluvium	Phonolitic pyroclasts	Phonolitic pyroclasts	Phonolitic pyroclasts
Field Reference	2-BRV	7-BRV	8-BRV	28-BRV	29-BRV	18-BRV	31-BRV	32-BRV	40-BRV
X	747105	741894	741631	746947	747053	744631	746158	746421	746789
Y	1641368	1644210	1644210	1639789	1639736	1642579	1643684	1643736	1645421
Altitude	600	80	50	430	430	650	790	780	475
Granulometry $\phi < 50 \mu\text{m}$ (%)	60.0	22.0	44.0	20.0	20.0	26.0	67.0	46.0	57.0
Munsell Color (Munsell, 1998)	Yellowish red 5 YR (4/6)	Dark Yellowish brown 10 YR (4/4)	Dark Yellowish brown 10 YR (3/4)	Dark Yellowish brown 10 YR (4/4)	Dark Yellowish brown 10 YR (4/4)	Brown 7.5 YR (4/4)	Dark Yellowish brown 10 YR (4/6)	Yellowish brown 10 YR (5/4)	Brown 7.5 YR (4/4)

Table 2. Sample references, and chemical composition of the clay-size fraction of topsoils from Brava Island (Cape Verde).

(major elements in % w/w, and trace elements in mg/kg)

Field Reference (size fraction)	2-BRV (< 2 μm)	7-BRV (< 2 μm)	8-BRV (< 2 μm)	28-BRV (< 2 μm)	29-BRV (< 2 μm)	18-BRV (< 2 μm)	31-BRV (< 2 μm)	32-BRV (< 2 μm)	40-BRV (< 2 μm)
Na ₂ O	0.418	0.743	0.446	1.88	0.356	2.37	2.02	1.32	1.25
K ₂ O	1.14	2.26	2.49	1.56	1.63	1.61	2.22	2.32	3.44
Fe ₂ O ₃ T	11.1	12.1	10.1	5.93	6.10	8.99	8.69	7.92	9.30
Sc	20.6	21.9	21.0	6.47	7.08	11.5	12.3	11.1	16.1
Cr	34.5	54.1	69.8	40.8	50.0	41.8	52.5	40.5	64.3
Mn	2742	2927	3477	4662	5615	7489	3291	3501	4236
Co	36.9	64.0	42.4	25.4	24.9	19.0	17.6	17.7	27.5
Zn	124	209	305	332	376	588	387	335	518
Ga	35.2	28.4	30.4	45.5	27.4	49.6	50.6	41.7	38.1
As	4.87	4.90	4.97	2.81	3.53	7.65	6.98	4.81	4.50
Br	22.3	36.7	36.5	26.0	17.2	27.3	62.8	30.4	33.2
Rb	65.0	91.8	123	66.2	77.5	117	121	108	102
Zr	673	462	463	402	441	783	1699	1010	333
Sb	0.288	12.5	0.487	0.319	0.334	0.530	28.1	6.50	14.3
Cs	1.58	3.00	4.36	2.52	2.86	3.32	4.81	3.05	3.71
Ba	1703	439	521	1989	1476	2484	737	1021	895
La	166	83.2	97.6	508	524	1260	226	291	194
Ce	417	211	248	696	691	1568	311	524	305
Nd	130	85.8	79.2	274	289	657	124	159	116
Sm	19.1	13.9	13.0	41.0	44.3	62.9	16.8	21.8	17.6
Eu	6.00	4.06	3.33	12.4	12.4	19.3	5.09	6.43	4.97
Tb	2.33	1.61	1.49	4.61	4.94	5.10	1.79	2.27	1.97
Yb	5.37	3.87	4.37	11.0	11.6	12.3	5.87	5.77	4.56
Lu	0.751	0.521	0.515	1.26	1.33	1.56	0.766	0.703	0.577
Hf	13.4	8.12	8.74	4.52	4.80	10.2	28.0	17.3	6.94
Ta	4.52	4.40	4.51	1.80	2.24	2.96	7.10	5.03	3.78
W	2.79	2.17	3.15	5.05	4.08	4.05	4.14	3.32	2.61
Th	18.4	11.7	15.4	18.7	19.9	48.3	34.3	28.5	16.4
U	2.49	2.61	2.97	3.87	3.23	5.98	6.37	3.60	3.36

Table 2. Estimated parameters from the Mössbauer spectra, taken at different temperatures, of the clay-size fraction of Brava Island topsoil samples.

Sample reference	T		IS, mm/s	QS, ϵ , mm/s	B_{hf} , tesla	Γ , mm/s	I	%Fe _{nso}
29-BRV	295 K	Fe ³⁺ nso/silicate	0.38	0.74	-	0.48	100%	
	4 K	Fe ³⁺ silicate Fe ³⁺ nso	0.50 0.52 0.49	0.71 -0.19 -0.04	- 49.5 46.6	0.74 0.63 0.57	15% 23% 62%	85%
8-BRV	295 K	Fe ³⁺ nso/silicate	0.36	0.66	-	0.55	100%	
	4 K	Fe ³⁺ silicate Fe ³⁺ nso	0.47 0.48 0.48	0.63 -0.19 -0.07	- 50.7 46.0	0.65 0.45 0.90	41% 34% 25%	59%
28-BRV	295 K	Fe ³⁺ nso/silicate	0.37	0.70	-	0.55	100%	
		Fe ³⁺ silicate Fe ³⁺ nso	0.47 0.50 0.48	0.65 -0.19 -0.20	- 50.0 44.9	0.72 0.62 0.61	38% 53% 9%	62%
29-BRV	295 K	Fe ³⁺ nso/silicate	0.37	0.69	-	0.56	100%	
	4 K	Fe ³⁺ silicate Fe ³⁺ nso	0.46 0.48 0.48	0.69 -0.19 -0.06	- 50.1 45.8	0.69 0.56 0.49	36% 44% 20%	64%
32-BRV	295 K	Fe ³⁺ nso/silicate	0.37	0.72	-	0.52	100%	
	4 K	Fe ³⁺ silicate Fe ³⁺ nso	0.46 0.47 0.50	0.68 -0.20 -0.04	- 50.0 46.5	0.73 0.73 0.68	30% 14% 56%	70%
18-BRV	295 K	Fe ³⁺ nso/silicate	0.37	0.70	-	0.53	100%	
	4 K	Fe ³⁺ silicate Fe ³⁺ nso	0.47 0.49 0.49	0.67 -0.19 -0.02	- 49.9 46.4	0.75 0.46 0.77	26% 31% 43%	74%
31-BRV	295 K	Fe ³⁺ nso/silicate	0.37	0.73	-	0.53	100%	
	4 K	Fe ³⁺ silicate Fe ³⁺ nso	0.48 0.48 0.49	0.65 -0.20 -0.03	- 50.1 46.5	0.68 0.51 0.64	20% 26% 54%	80%
40-BRV	295 K	Fe ³⁺ nso/silicate	0.38	0.72	-	0.57	100%	
	4 K	Fe ³⁺ silicate Fe ³⁺ nso	0.47 0.47 0.50	0.63 -0.19 -0.04	- 50.9 46.7	0.75 0.51 0.88	36% 26% 39%	64%

nso – nanosized Fe oxides which are superparamagnetic at room temperature

%Fe_{nso} fraction of the total Fe in the topsoil incorporated in Fe³⁺ oxides

IS (mm/s) – isomer shift relative to α -Fe at 295 K; QS (mm/s) – quadrupole splitting and ϵ (mm/s) – quadrupole shift estimated for quadrupole doublets and magnetic sextets, respectively.

B_{hf} (tesla) – magnetic hyperfine field; I – relative area. Estimated errors are ≤ 0.02 mm/s for IS, QS, ϵ , < 0.2 T for B_{hf} and $< 2\%$ for I.